A Modified Multiphase Oscillator with Improved Phase Noise Performance

Antonie C. Alberts[1], Saurabh Sinha[1,2]

[1]*Carl and Emily Fuchs Institute for Microelectronics, Department of Electrical, Electronic and Computer Engineering, University of Pretoria, Pretoria, South Africa*

[2]*Faculty of Engineering and Built Environment, University of Johannesburg, Johannesburg, South Africa*

Abstract

This paper investigates the factors that influence the phase noise performance of an oscillator and proposes a modified structure for improved phase noise performance. A single and multiphase oscillator analysis using the harmonic balance method is presented. The modified structure increases the oscillation amplitude without increasing the bias current and leads to improved phase noise performance as well as decreased power consumption. The modification is analyzed and the figure of merit of the oscillator shows a significant improvement of 21 dB. Numerical and analytical solutions are presented to predict the oscillation frequency and phase noise. The analytical solution is used to approximate the first harmonic and can be combined with numerical simulations to extrapolate phase noise performance.

Keywords: harmonic analysis, oscillators, phase noise, SPICE.

1   Introduction

Oscillators are ubiquitous to radio frequency circuits, where frequency translations and channel selection play a central role in the analog communications channel. Oscillators also form part of digital systems as a time reference [1]. Typical heterodyne receivers require an intermediate frequency channel. The associated oscillators and variable filters can only be centered perfectly at a single frequency and degrade performance at the boundaries of the channel. These circuits also require image-rejecting filters and phase-locked loops to enable down-conversion. The penalty for these components is increased circuit area and power consumption [2]. A direct down-conversion circuit will enable the number of components in the system to be reduced. A requirement added by the structural change is a passive sub-harmonic mixer. Quadrature oscillators can be achieved by cross-coupling two nominally identical LC differential voltage-controlled

oscillators (VCOs) [3]. Because of the widespread use of VCOs in wireless communication systems, the development of comprehensive nonlinear analysis is of great interest for both theory and applications [4]. A key characteristic that defines the performance of an oscillator is the phase noise measurement and extensive work has been done to quantify phase noise. The VCO is also a key component in phase-locked loops and will contribute to most of the out-of-band phase noise, as well as a significant portion of in-band noise [5]. Current state-of-the-art modulation techniques, implemented at 60 GHz, such as quadrature amplitude modulation and orthogonal frequency domain multiplexing, require phase noise specifications better than 90 dBc/Hz at a 1 MHz offset [6]. It has been shown that owing to the timing of the current injection, the Colpitts oscillator tends to outperform other oscillator structures in terms of phase noise performance [7]. The Colpitts oscillator has a major flaw in that the startup gain must be relatively high when compared to the cross-coupled oscillator. The oscillation amplitude cannot be extended as in the cross-coupled case [8]. The oscillation amplitude is generally limited by the oscillator's bias current and is given as $\dfrac{2I_P R_{\text{tank}}}{\pi}$ [9]. The phase noise is defined by a stochastic differential equation, which can be used to predict the system's phase noise performance. The characteristics of the oscillator can then be defined using the trajectory. The model projects the noise components of the oscillator onto the trajectory and then translates the noise into the resulting phase and amplitude shift [10]. The phase noise performance of an oscillator can be improved by altering the shape of the trajectory. The trajectory of the oscillator can be separated into slow and fast transients. The phase noise performance can be improved by improving the shape of the slow manifold of the oscillator [11]. Close-in phase noise can be directly improved by improving the loaded quality factor of the tank circuit [12]. The Colpitts and differential Colpitts oscillator are selected as the basis for analyzing performance. The organization and contribution of this paper are as follows: In Section II the factors that influence phase noise are discussed; the results are compared to a system where the non-linear restorative force has been omitted to produce closed form solutions. Several characteristics influencing phase noise are identified. In Section III, a simple single-phased Colpitts oscillator is analyzed. The analysis is based on the harmonic balance technique and is analytically extracted for the first Fourier component, which is simultaneously estimated. This method can be extended for higher order harmonics [13]. The approximate frequency–amplitude relationship for a conservative nonlinear oscillatory system in which the restoring force has an exponential form is studied. The solutions are valid for the complete range of oscillation amplitudes, including limiting cases of amplitudes approaching zero and infinity. The analysis used in this paper produces accurate results because of the large number of harmonics that are explained using this technique [13]. Modified nodal analysis is used to determine the differential

system describing the oscillator. The set of equations is non-linear and a closed form solution does not exist. The oscillation frequency and amplitude can be fully explained using this technique, and an approximation of the first harmonic component is made. The transistor is modeled using the full voltage-controlled Ebers-Moll bipolar junction transistor model. Section IV extends the approach discussed in Section III to a differential Colpitts oscillator. This structure is then used as the basis for the improved multiphase oscillator. The section shows the subtle difference between this structure and the cross-coupled oscillator. Section V introduces the modified multiphase oscillator with analysis to predict the oscillation amplitude and frequency. This is verified through a MATLAB simulation of the describing differential equation, which can be done either in the time domain or in the frequency domain, using a numerical harmonic balance procedure. The time domain approach tends to generate less accurate solutions and is more computationally expensive. Section VI provides a brief discussion on the phase noise of the oscillator. Finally the multiphase oscillator is analyzed. A general simulation program with integrated circuit emphasis (SPICE) solution is also compared in order to verify the analysis. A new oscillator structure is introduced with current locking to enable the generation of quadrature oscillations. The structure takes advantage of the noise-shaping characteristics of the Colpitts oscillator but relaxes the start-up requirements associated with the structure. The result is a multiphase oscillator with reduced power consumption and improved phase noise performance.

2 Oscillator performance

The phase noise of an oscillator can be improved without difficulty by increasing the amplitude of the oscillating voltage and the power associated with the first harmonic, or by improving the quality factor of the tank circuit. These methods are well noted [14]. There are limitations to both of these approaches and it is useful to define a performance metric for the oscillator. The figure of merit (FOM) is defined as follows:

$$\text{FOM} = \mathcal{L}(\Delta f) - 20\log\left(\frac{f_0}{\Delta f}\right) + 10\log\left(\frac{P_{DC}}{1\text{mW}}\right) \tag{1}$$

where $\mathcal{L}(\Delta f)$ is the phase noise at a Δf offset frequency in dBc/Hz, f_0 is the oscillation frequency and P_{DC} is the steady state power consumption of the circuit in Watts(1). From (1) it is clear that there are two ways to improve the FOM: improve the phase noise *or* decrease the power consumption of the oscillator. Phase noise has been shown to be stationary

and to have increasing variance with time. The total power of the circuit is defined by (2).

$$P_{tot} = \sum_{i=1}^{\infty} |X_i|^2 \tag{2}$$

where X_i are the Fourier components of the oscillator's stable limit cycle in volts squared relative to a 1 Ω load. The phase noise is then given as:

$$\mathcal{L}(\Delta f) = 10 \log_{10} \left(\frac{S_{ss}(f_0 + \Delta f)}{2|X_1|^2} \right), \tag{3}$$

and $S_{ss}(f_0 + \Delta f)$ is the power spectral density in W/Hz, at a frequency offset of Δf Hz. The result of (1) and (2) is that phase noise can be reduced by decreasing the total number of harmonics within the system. The total energy of the system is limited and the summation of all the components must be equal to the steady state power consumption. To identify methods of reducing phase noise one needs to analyze how noise perturbations are translated into phase noise in an autonomous system. Equations (4) and (5) give one a basis to begin analyzing phase noise and identify methods that can be used to reduce phase noise. The phase noise of a circuit with stationary noise sources is then approximately:

$$\mathcal{L}(\Delta f) \approx 10 \log_{10} \left(\frac{f_0^2 c}{\pi^2 f_0^4 c^2 + \Delta f^2} \right), \tag{4}$$

for small c, $0 \le \Delta f << f_0$ and

$$c_i = \frac{1}{T} \int_0^T v_1^T(\tau) B(x_s(\tau)) B^T(x_s(\tau)) v_1(\tau) d\tau, \tag{5}$$

where c_i is the function that describes a noise source i and c is the sum of all the noise source contributions. Equation (5) is the projection of the noise, assumed stationary, described by $B(x_s(\tau))$ and a function of $x_s(\tau)$ onto the trajectory of the specific node of the system without the presence of noise. It then describes how the noise source is translated into phase noise. The FOM can therefore be improved by reducing the constants, c_i. This can be achieved in two ways, by manipulating the manner in which noise is translated into phase noise or by reducing noise within the system. Initially it

4

was shown that to calculate the phase noise of an oscillator, the noise at each node should be projected in the relative state space to the node of interest to predict phase noise. A description of calculating phase noise is given in [1]. The theory is then later expanded to show that only a single variable in the state space is required to obtain the relevant perturbation projection vector (PPV) [16]. The tank current is equivalent to the first derivative of the tank voltage and can be seen as a function of the rate of change of phase. This enables noise sources that are in the form of current perturbations to be directly analyzed, with the PPV being the tangent of the limit cycle. This corresponds directly with the idea of an impulse sensitivity function introduced [7]. The assumption is that the noise is a wide sense stationary variable. The case of colored noise sources is considered in [10]. An interesting analysis, which is conducted in [17], is similar to the method presented here. In this work a lower-order active device is included as the restorative element for the lossy tank circuit and enables subtle differences to be included. In [17], the active device is removed from the model and approximated with an ideal switch, which is mathematically tractable. The currents from the ideal switches are then injected into a tank circuit as impulses and the PPV is calculated exactly under the listed assumptions. The ideal switch tends to approximate the cross-coupled transistors as the gain of the active transistor is taken in the limit to infinity, although this is only true for the basic configuration. This yields results that agree with "intuitive" selection of the oscillator structure. The results highlight a few important aspects. The optimum difference between the eigenvectors representing the current and voltage of the tank circuit is $\frac{1}{2}\pi$. This then results in the sensitivity of noise-to-phase-noise conversion being minimized when the voltage and current are out of phase and the voltage is at a maximum. This corresponds directly with the Colpitts oscillator where the current injection is out of phase with the oscillation voltage. Secondly, the coefficient describing the PPV onto the current variable in the state space is given as:

$$\frac{1}{F} = \sqrt{\frac{L}{C}} \sqrt{1 + \frac{1}{(2Q)^2}} \, , \tag{6}$$

where F describes how the components of the tank circuit will contribute to the PPV of the noise current sources. The interesting result here is the fact that an increased Q will improve phase noise, as stated before. The ratio of C to L will also influence phase noise. Finally, by considering the slow transients of the system, the manifold can be analyzed and the shape of the

5

PPV relative to specific state variables in the slow manifold can be manipulated to improve phase noise.

3 Modelling oscillators for analysis

3.1 Single-phase Colpitts oscillator

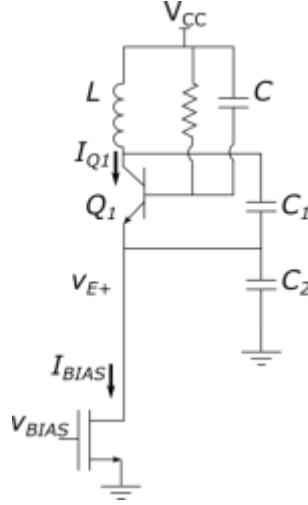Figure 1 shows the basic Colpitts oscillator. Equation (7) is the result of nodal analysis.

Figure 1. Basic Colpitts oscillator.

$$i_{Q1+} + \frac{\int_{-\infty}^{t}\left(v_+(\tau)-V_{CC}\right)\partial\tau}{L} + C_{tot}\frac{\partial v_{1+}}{\partial t} + \frac{\left(v_+(\tau)-V_{CC}\right)}{R_P} = 0 \tag{7}$$

where i_{Q1+} is the collector current of Q_1, v_+ is the tank voltage with respect to ground, C_{tot} is the total capacitance associated with the tank circuit. After applying the Ebers-Moll equations for the transistor collector current, (8) is derived.

$$\frac{\partial^2 v_+}{\partial t^2} + \frac{\partial v_+}{C_{tot}R_p\partial t} + \frac{\partial\left(I_s\left(\exp\left(\frac{v_{BE}}{V_T}\right) - \frac{1}{\alpha_R}\exp\left(\frac{v_{BC}}{V_T}\right)\right)\right)}{C_{tot}\partial t} + v_+(\tau)\left(\frac{1}{C_{tot}L}\right) = 0 \tag{8}$$

where v_{BE} and v_{BC} represent the base-emitter and base-collector voltages of Q_1 respectively. This equation then resembles the Van der Pol equation,

6

which has been extensively studied [19]. Equation (8) does not have an explicit closed form solution.

The equation is simplified (see Appendix A) to yield (9).

$$\left(\left(\left(\frac{1}{C_{tot}L}\right)-\omega^2\right)+\left(\frac{-\omega}{C_{tot}R_P}+\left(\frac{I_s\exp\left(\frac{V_B}{V_T}\right)\omega}{C_{tot}}\right)\times\left(\sum_{n=0}^{\infty}\left(K_1\left(K_1A\right)^{2n}\left(\frac{1}{2^{2n}}\frac{1}{\left((2n)!\right)^{2n}(n+1)!n!}\right)\right)\right)\right)\right)=0$$

(9)

The oscillation frequency can also be dramatically increased from the third term, $\dfrac{-\omega}{C_{tot}R_P}$ in (9), when the feedback constant is small and the loaded tank quality is small, before the last term dominates and reduces oscillation frequency. The term R_P is frequency-dependent; its effects are initially deliberately excluded from the analysis, but will tend to change the oscillation frequency. To deal with these effects, the assumption is made that the analysis is based on the fact that the tank circuit is insignificantly loaded by the feedback network. The objective is then to place the oscillator on the verge of being voltage-limited and the amplitude can be set as the limit defined by the bias; in this example it is ½V_{CC}. To calculate the loading on the circuit, the authors rely on the defined set of assumptions that the first harmonic's current is set by the modified Bessel function defining the Fourier transform of the function $\exp(x\cos(t))$. The transconductance of the first harmonic is well known to be $2I_{BIAS}/V_T$. This then allows the loaded impedance of the tank circuit to be defined as $Z_P(\omega)\|\left(\dfrac{V_T}{2I_{BIAS}}n^2\right)$, at the first harmonic. The dependence of the impedance on frequency is not limiting and (9) can be iteratively analyzed until the equations are balanced. To limit the frequency deviations the non-linearity should be kept small and the tank impedance as large as possible. The limitation to (9) is the assumption that the combination of C_1 and C_2 does not load the tank circuit. This assumption allows the base-emitter voltage to be expressed as a fraction, defined by n, of the tank voltage. The assumptions are therefore valid for large values of n, as well as for small bias currents where the impedance into the emitter is larger than the tank impedance. The factors

that influence phase noise and the assumption that the tank is not significantly loaded by the feedback circuit lead to the false assumption that the oscillation amplitude and bias currents cannot be separated. The theory states that if the bias current is reduced, the oscillation amplitude must decrease. This result can be verified with most feedback oscillators. The two are in fact not necessarily inter-dependent and can be decoupled if an external current is injected into the emitter of the active transistor. First it will be demonstrated that the assumption that the first harmonic is limited by bias current is not necessarily true. Starting with the circuit in Fig. 1 and (7), another state variable is included in the form of v_E, the emitter voltage. Firstly, it is assumed that the transistor β is large and the transistor emitter and collector currents can be interchanged. This is only true if the transistor is in saturation, which could be violated and should be verified not to be so in each specific case. Equation (7) can be modified to:

$$i_{Q1+} + \frac{\int_{-\infty}^{t}\left(v_+(\tau)-V_{CC}\right)\partial\tau}{L} + C_1\frac{\partial\left(v_{1+}-v_E\right)}{\partial t} + \frac{\left(v_+(\tau)-V_{CC}\right)}{R_P} = 0 \qquad (10)$$

and the additional node added to obtain the following sets of equations:

$$i_E - I_{CONST} - \frac{C_2\partial v_E}{\partial t} - \frac{C_1\partial\left(v_E-v_+\right)}{\partial t} = 0 \qquad (11)$$

$$2i_{Q1+} + \frac{\int_{-\infty}^{t}\left(v_+(\tau)-V_{CC}\right)\partial\tau}{L} - I_{CONST} - \frac{C_2\partial v_E}{\partial t} + \frac{\left(v_+(\tau)-V_{CC}\right)}{R_P} = 0 \quad (12)$$

$$\left(\frac{2I_S\left(-\frac{\partial v_E}{\partial t}\right)}{V_T}\exp\left(\frac{K-v_E}{V_T}\right)\right) - \frac{C_2\partial v_E{}^2}{\left(\partial t\right)^2} + v_+\left(\frac{1}{L}+\frac{1}{R_P}\right) = 0$$

$$(13)$$

$$v_+ = \left(L\,\|\,R_P\right)\left(\frac{C_2\partial^2 v_E}{\left(\partial t\right)^2} + \frac{2I_s\left(\frac{\partial v_E}{\partial t}\right)}{V_T}\exp\left(\frac{K-v_E}{V_T}\right)\right) \qquad (14)$$

$$\frac{\partial v_E}{\partial t}\left(C_1+C_2\right) = C_1\frac{\partial v_1}{\partial t} + I_S\exp\left(\frac{V_B-v_E}{V_T}\right) - I_{CONST}. \qquad (15)$$

8

After some manipulation (see Appendix B) we arrive at

$$\left(\frac{A}{L\parallel R_P}+C_2 A_1 \omega^2\right)\cos\left(\omega t\right)=$$

$$P\omega\left[\left(A_1\left(T_1 T_2\right)\right)+\left(A_2 T_2 T_3\right)-A_2 T_4 T_1 - A_2 T_5 T_1 -\left(\frac{A_1}{4}\right)T_6 T_4 +\left(\frac{A_1}{4}\right)T_6 T_5\right]\sin\left(\omega t\right)+ \qquad (16)$$

$$P\omega\left(\frac{A_2}{2}T_6 T_4 +\frac{A_2}{2}T_6 T_5 - A_2 2 T_2^2 +\left(\frac{A_1}{2}T_1 T_3\right)-\frac{A_1}{2}T_4 T_2 -\frac{A_1}{2}T_5 T_2\right)\sin\left(2\omega t\right)$$

Equation (16) can be used to predict the oscillation frequency as well as the values of A_1 and A_2, the amplitude of the first and second harmonic component of the oscillator. Increasing the ratio $\left(\dfrac{C_2}{C_2 + C_1}\right)$ will increase the amplitude of the first harmonic of the collector current, if the tank circuit is not significantly loaded, which is not true for the general oscillator. The structure must be modified to allow the tank loading to be decoupled from the feedback ratio. The results show that if the small loop gain can be set to ensure oscillation begins, the average collector current can be reduced after oscillation begins, or if the closed loop gain is increased the bias current can be reduced, by almost the same factor. Equation (16) shows that for large quality factors the oscillation frequency will decrease rapidly as the number of harmonics in the feedback voltage is increased. The number of harmonics in the feedback voltage is not related to the number of harmonics present in the tank, but rather the amplitude of the feedback voltage.

3.2   Differential Colpitts oscillator
The single-phase Colpitts oscillator is modified. Two tank circuits are coupled and forced to oscillate out of phase. The modification is shown in Fig. 2.
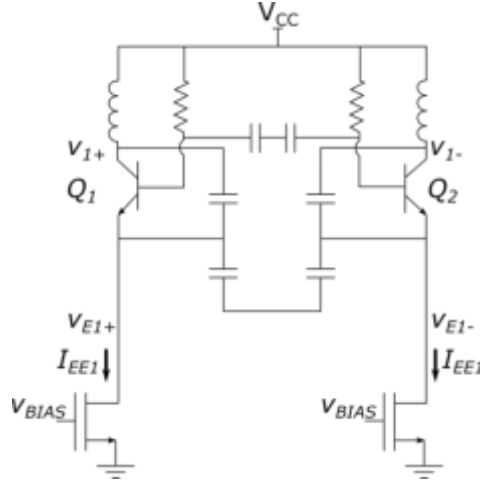
Figure 2. Differential Colpitts oscillator.

The two coupled single-phase Colpitts oscillators are identical. Nodal analysis leads to (17) and (18):

$$v_{E1+} + v_{B1+} - v_{B1-} + v_{E1-} = 0 \, , \tag{17}$$

$$v_{B1+} - v_{E1+} = V_T \ln\left(\frac{i_{C1+}}{I_{S1}}\right) \, , \tag{18}$$

where i_{C1+} is the collector current of Q_1. I_{S1} is the saturation current. V_T is the thermal voltage, v_{B1+} and v_{B1-} are the base voltages of Q_1 and Q_2 respectively. Then, applying the same steps as before, it can be shown that

$$\left(i_{C1+} - i_{C1-}\right) + \frac{\int_{-\infty}^{t}\left(v_{1+}(\tau) - v_{1-}(\tau)\right)\partial\tau}{L} + C_{tot}\frac{\partial\left(v_{1+} - v_{1-}\right)}{\partial t} + \left(i_{2+} - i_{2-}\right) = 0 \, . \tag{19}$$

The collector current is set by the base-emitter voltage of the particular transistor. The currents can be further expanded and the result is shown in (19):

$$\frac{\partial\left(-I_s \exp\left(\frac{V_{B+}}{V_t}\right)\left(\sinh\left(\frac{-\left(\frac{C_2}{C_1+C_2}v_{1D}\right)}{2V_t}\right)\right)\right)}{\partial t} + \frac{v_{1D}}{L} + C_{tot}\frac{\partial^2 v_{1D}}{\partial t^2} = 0 \tag{20}$$

10

where v_{1D} is the differential voltage across both tank circuits. Then, applying the partial derivative, it can be shown that:

$$\frac{\partial^2 v_{1D}}{\partial t^2} + \frac{\left(\left(-I_s \exp\left(\frac{V_{B+}}{V_t}\right)\right)\left(\cosh\left(\frac{-\left(\frac{C_2}{C_1+C_2} v_{1D}\right)}{2V_t}\right)\right)\right)}{\partial t C_{tot}} \times \left(\frac{-\left(\frac{C_2}{C_1+C_2}\right)}{2V_t}\right)\left(\frac{\partial v_{1D}}{\partial t}\right) + \frac{v_{1D}}{C_{tot}L} = 0$$

(21)

The system is expanded as a set of first-order differential equations:

$$\frac{\partial v_{1D}}{\partial t} = x_1$$

(22)

$$\frac{\partial x_1}{\partial t} = Q.K\left(\cosh\left(Kv_{1D\angle G}\right)\right) \times \left(x_{1\angle G}\right) - \frac{v_{1D}}{C_{tot}L}$$

(23)

where $Q = \dfrac{-I_s \exp\left(\dfrac{V_{B+}}{V_t}\right)}{C_{tot}}$, $K = \left(\dfrac{-\left(\dfrac{C_2}{C_1+C_2}\right)}{2V_t}\right)$; using these equations, a numerical

solution for the differential equation can be derived. The equation can also be used directly to generate phase plots for the system. With algebraic manipulation, using the same harmonic balance technique given in the previous section, an approximate closed form solution defining the oscillation frequency and amplitude can be derived.

3.3 Multiphase Colpitts oscillator

The currents of two differential Colpitts oscillators are cross-coupled to enable the generation of a quadrature oscillator. When the two differential tank circuits are coupled the result is a 90° shift in the differential voltages and four oscillations that are separated by equal phases are generated [18]. The modified Colpitts oscillator is shown in Fig. 3 and Fig. 4. An additional gain stage is introduced into the feedback loop. This enables the start-up conditions associated with the Colpitts oscillator to be altered. The tank circuits of each of the oscillators' branches are decoupled from the feedback

11

loop. This separation allows the loaded quality factor of the relative tank circuit to be improved. The closed-loop gain is also increased. When the modified circuits describing equations are analyzed, it can be seen how the feedback voltage is increased. This simultaneously increases the tank voltage. The oscillator is designed to enable the feedback voltages at the base of transistors Q_2, Q_3, Q_8, and Q_9 to be smaller than 50 mV, which enables small-signal linear analysis of the gain to be applied. The additional components used to modify the quadrature oscillator increase the space required to implement the oscillator. The increase in size is in line with other quadrature oscillators implemented with similar technology nodes, such as the transformer coupled and travelling wave oscillators. The layout complexity is however significantly increased and interconnection becomes more challenging. There is also a further assumption that the additional gain stage introduced into the oscillator structure does not introduce large phase deviations. This can be ensured in the design phase; however if care is not taken, subharmonic or superharmonic oscillations as well as frequency pulling will occur. The modification improves the phase noise performance by exploiting several different facts. The bias currents required to ensure start-up of the oscillators are reduced and a very low power oscillator can be realized. The ratio of the capacitors C_1 and C_2 can be increased by approximately the same factor as the gain added to the feedback loop. The loaded quality factor of the tank circuit is improved. The cross-coupled voltages remain equivalent to the unmodified system, leaving the harmonic content of the tank circuit unaffected. The current injections into the tank circuit are optimum in terms of the $\frac{1}{2}\pi$ shift between the current and voltage. The noise contribution to the tank circuit is reduced by careful selection of the gain block parameters. The remaining noise components are set by the specific process and the quality of the passive components. Thus the modifications proposed aim to improve every aspect identified to have an influence on the oscillators' phase noise performance, except for device and component level optimizations. The gain of the transistors Q_1, Q_4, Q_7, and Q_{10} is set to 18 dB to optimize the phase noise of the oscillator. The emitter voltages are then defined by the following equations:

$$v_{E1+} = -8.5\left(\frac{C_2}{C_2 + C_1}\right)v_{1-}\angle G$$

(24)

$$v_{E1+} = -8.5\left(\frac{C_2}{C_2 + C_1}\right)v_{1-}\angle G$$

(25)

$$v_{E1-} = -8.5\left(\frac{C_2}{C_2 + C_1}\right)v_{1+}\angle G$$

$$(26)$$

$$v_{E2+} = -8.5\left(\frac{C_2}{C_2 + C_1}\right)v_{2-}\angle G$$

$$(27)$$

$$v_{E2-} = -8.5\left(\frac{C_2}{C_2 + C_1}\right)v_{2+}\angle G$$

$$(28)$$

where $\angle G$ is the phase shift associated with the gain stage. Then, collecting the terms and defining the differential voltages and currents, equations (29) and (30) can be derived.
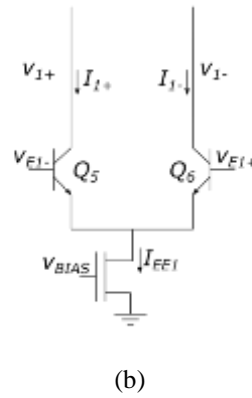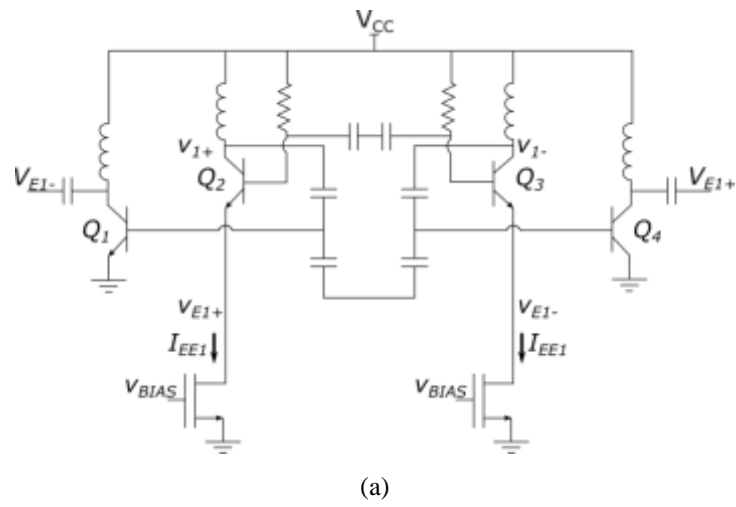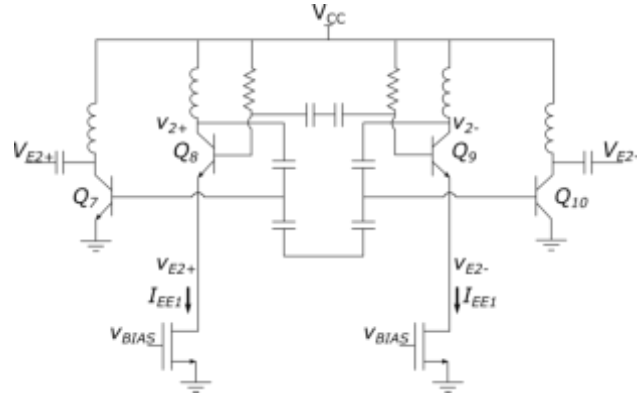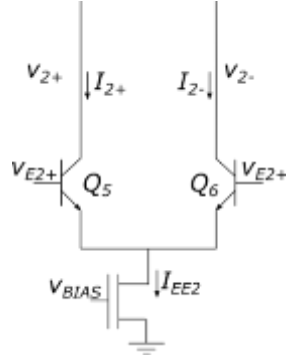

(a)

(b)

Figure 3. Multiphase Colpitts oscillator.

(a)

(b)

Figure 4. Multiphase Colpitts oscillator.

$$\frac{\partial i_{CD1}}{\partial t} + \frac{v_{1D}}{L} + C_{tot} \frac{\partial^2 v_{1D}}{\partial t^2} + \frac{\partial i_{2D}}{\partial t} = 0 \tag{29}$$

$$\frac{\partial i_{CD2}}{\partial t} + \frac{v_{2D}}{L} + C_{tot} \frac{\partial^2 v_{2D}}{\partial t^2} - \frac{\partial i_{1D}}{\partial t} = 0 \tag{30}$$

where $i_{CD1} = i_{C1+} - i_{C1-}$, $i_{CD2} = i_{C2+} - i_{C2-}$, $v_{1D} = v_{1+} - v_{1-}$, $v_{2D} = v_{2+} - v_{2-}$, $i_{1D} = i_{1+} - i_{1-}$, and $i_{2D} = i_{2+} - i_{2-}$.

Then, after several algebraic steps, if $K = \dfrac{8.5C_2}{2V_t\left(C_1 + C_2\right)}$, $A = \dfrac{2\alpha_F I_{EE2}}{C_{tot}}$,

$x_1 = \dfrac{\partial v_{1D}}{\partial t}$, $x_2 = \dfrac{\partial v_{2D}}{\partial t}$, $Q = -I_s \exp\left(\dfrac{V_{B+}}{V_t}\right)$ it can be shown that:

$$\frac{\partial v_{1D}}{\partial t} = x_1 \tag{31}$$

$$\frac{\partial v_{2D}}{\partial t} = x_2 \tag{32}$$

$$\frac{\partial x_1}{\partial t} = Q.K\left(\cosh\left(Kv_{1D\angle G}\right)\right)\times\left(x_{1\angle G}\right) + P.A.K\left(1 - \tanh^2\left(Kv_{2D\angle G}\right)\right)\times\left(x_{2\angle G}\right) - \frac{v_{1D}}{C_{tot}L} \tag{33}$$

$$\frac{\partial x_2}{\partial t} = Q.K\left(\cosh\left(Kv_{2D\angle G}\right)\right)\times\left(x_{2\angle G}\right) + P.A.K\left(\tanh^2\left(Kv_{1D\angle G}\right) - 1\right)\times\left(x_{1\angle G}\right) - \frac{v_{2D}}{C_{tot}L} \tag{34}$$

This reflects the modified nodal analysis, which can then be used to solve the system numerically. It is interesting to note that in the conventional cross-coupled pair the terms with the hyperbolic sine are replaced with the tanh function, which demonstrates how the maximum gain is no longer restricted. This is the only mathematical difference between the two circuits. The magnitude of the cross-coupled currents is important in terms of the performance of the system and should be set at a minimum while still ensuring quadrature oscillations. An added benefit of the additional gain block becomes apparent when looking at (31) to (34), where it is seen that the cross-coupling of the currents is magnified for a given oscillation amplitude. The phase noise improvements are not specifically clear in the differential equation, but are clearer when looking at the bias currents and the 8.5 factor reduction that can be achieved with this specific configuration.

3.4 A brief analysis of phase noise

To characterize the phase noise in the oscillator, the phase error is defined at a given point in time as $\theta(t)$ - the following is then considered:

$$dif(t) = \left(A + \varepsilon(t)\right)\cos\left(t + \theta(t)\right) - A\cos(t), \tag{35}$$

where the phase shift is due to the injected error signal $dif(t)$, which causes an amplitude shift of $\varepsilon(t)$ and phase change, $\theta(t)$. $A\cos(t)$ is the

expected oscillator output given a noiseless system. The term $\varepsilon(t)$ will be reduced by the natural amplitude-limiting nature of the oscillator, which must be valid for a stable oscillatory system. To characterize the phase noise, the first and second order moments of the differential equations that define the system [1] are analyzed.

$$I(X,t)dt + dQ(X) + \varepsilon B(X,t)dW(t) = 0 . \tag{36}$$

The term $I(X,t)$ represents the linear and nonlinear resistive components of the system and $dQ(X)$ represents the inductive and capacitive components of the system. ε is a multiplier associated with perturbation theory, the factor $B(X,t)$ is a noise-modulating function and $W(t)$ is a vector of uncorrelated Wiener processes. The $E(X(t)) = x_s(t)$, which is the solution to (36) when the noise sources are ignored. The second order statistics are characterized by the autocorrelation function $E\left(X_n(t)X_n(t)^T\right)$, which is defined as $K(t)$. The second order statistics are solved around the known steady-state solution $x_s(t)$ and the Taylor expansion of $X(t)$ around the steady-state solution.

4   Numerical simulations

The differential equation (8) is solved numerically with the aid of MATLAB and generates $E(X(t)) = x_s(t)$; both a transient analysis and a shooting balance method are applied. The shooting balance method generates the state transition matrix and generates the Hessian required for calculating the phase noise using (36) and calculating $K(t)$. The component parameters are selected to match standard transistors available in a SPICE library. The tank circuit is loaded with a resistive component to reduce the quality factor of the tank circuit significantly to 10. This is done for demonstration purposes to increase the phase noise associated with the tank circuit. For the selected "standard" transistors, the I_S of the transistor is 10^{-17} A; the following selections are made: $V_B = 0.75$ V, $V_{CC} = 1.2$ V, $C_1/(C_1+C_2) = 0.35$, $1/(C_{tot}.L) = 10^{20}$, and $C_{tot} = 1$ pF and $R_p = 100 \ \Omega$ to intentionally reduce the tank circuits quality factor significantly. This yields an oscillation frequency

estimate of 5.03 MHz for the standard approximation, (14) yields 1.59 GHz. A lower frequency oscillator is demonstrated. The oscillation frequency is then 1.59 GHz, compared to the SPICE result of 1.6 GHz. Fig. 4 shows the multiphase oscillator. The current injection in Fig. 5 shows the 90° phase shift of the current injection relative to the tank current; the tank current and voltage must be out of phase. It is clear from Fig. 6 that the stable limit cycle is more strongly influenced by noise during periods when the rate of change of current with respect to voltage is at its maximum and is influenced by the coupling currents that induce the quadrature oscillations. The modified nodal analysis is extended and the different noise sources are added to the model. Applying the same approach to the multiphase Colpitts oscillator (24) using a larger tank capacitance and smaller DC bias, and setting the cross-coupling currents to 0.039 times the main oscillator's current results in Fig. 5 to Fig. 8. The noise sources are modeled as stationary sources with 0 mean and variance defined by the relative source characteristic projected to the tank node of the circuit. A Monte Carlo simulation is performed; the noise is added in the time domain and weighted appropriately. The results are compared to the expected value of the phase noise derived using the approach from [1] and [5]. The total power consumption of the oscillator is improved from 40.8 mW to 4.8 mW. Drawing comparisons to other quadrature oscillators manufactured in a similar process technology node yields: 50.4 mW for a ring oscillator [20], 24 mW for a parallel coupled oscillator [21] and 19.2 mW for a transformer coupled oscillator [22].

The additional gain stage is biased at a current of 1 mA and included in the power consumption of the total oscillator for comparison purposes. Fig. 7 shows the spectrum of the modified Colpitts oscillator. The phase noise is estimated to be -92 dBc at a 1 MHz offset, directly from the figure. The phase noise of the oscillator has not specifically been optimized. The analysis shows an improvement of approximately $20 \log_{10}(8.5)$ or a phase noise of -102 dBc at 1 MHz offset. The FOM is significantly improved by 21 dB. If the original oscillator were optimized the performance improvement would be reduced, but not more than 8 dB.
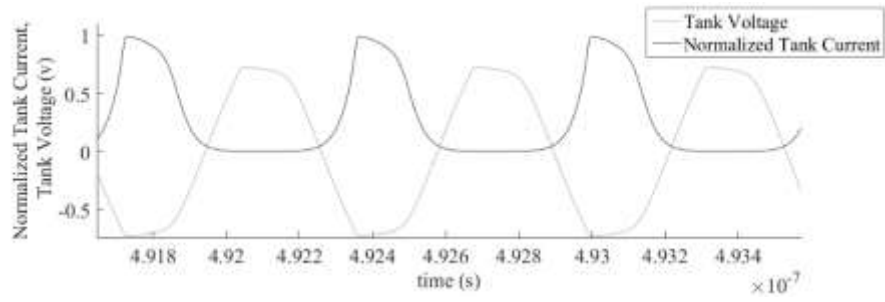
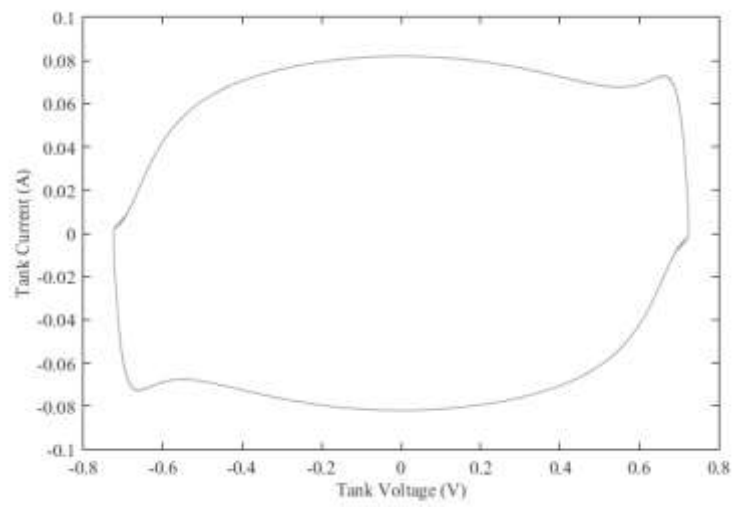Figure 5. Tank voltage versus transistor injection current for the multiphase oscillators.

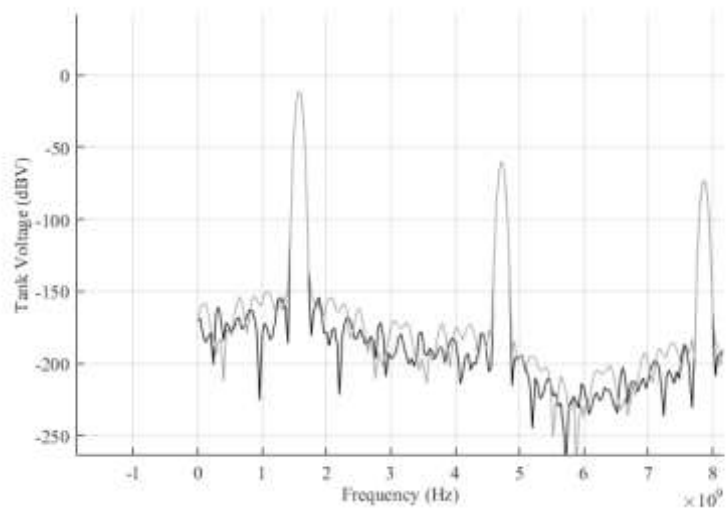Figure 6. Phase plot for the unmodified oscillator including noise.

Figure 7. Spectrum of oscillator and modified oscillator.

18

5 Conclusion

The approach followed in this paper describes oscillator behavior from a circuit level analysis. The derived equations do not have a closed form solution but are re-formulated using harmonic balance techniques to yield an approximate solution. The results from this closed form approximation are very close to both the numerical solutions of the differential equations as well as the SPICE solutions for the same circuits. The derived equations are able to predict amplitude and frequency in the single-phase example accurately and are extended to provide a numerical platform for defining the amplitude and frequency of a multiphase oscillator. The analysis identifies several different circuit components that influence the phase noise performance of an oscillator. A circuit level modification is then identified that enables some of the factors and their interactions to be decoupled. It is demonstrated that the phase noise performance of a Colpitts oscillator can be significantly improved by making the proposed changes to the oscillator. The FOM of the oscillator is improved even further. If it is considered that in most cases the collector current will account for approximately 85% of the phase noise, it is then clear that the methods proposed here will improve phase noise performance, for example from a given level of -106 dBc/Hz to -113 dBc/Hz. This would not account for further improvements the modification would incorporate in the limit cycle. The FOM would be improved even further by another 9 dB by the change in the power consumption relating to an average increase in performance of 16 dB. Future work could include further modeling of the phase shift in the feedback network, including the transmission lines in the feedback networks using the harmonic balance technique in a numerical form. The feedback technique can also be modified to be applicable to single and differential oscillators.

6   Appendix A

The truncated harmonic balance method is applied to equation (8). If

$$v = A\cos(\omega t), \quad \frac{\partial v}{\partial t} = -A\omega\sin(\omega t), \quad \text{and} \quad \frac{\partial^2 v}{\partial t^2} = -A\omega^2\cos(\omega t) \quad \text{then}$$

substituting into (8) yields:

$$-A\omega^2\cos(\omega t) + \frac{AK_1\omega\sin(\omega t)\times\left(K_2\exp\left(-K_1 A\cos(\omega t)\right)\right)}{C_{tot}}$$

$$-\frac{A\omega}{C_{tot}R_P}\sin(\omega t) + A\cos(\omega t)\left(\frac{1}{C_{tot}L}\right) = 0 \tag{A1}$$

where ω is the oscillation frequency, $K_1 = \dfrac{C_1}{V_T\left(C_1 + C_2\right)}$,

$K_2 = I_s\exp\left(\dfrac{V_B}{V_T}\right)$, and A is the oscillation amplitude. Equation (9) can be analyzed specifically for a given bias condition. The amplitude is limited by the saturation condition of the oscillator, with the maximum first harmonic oscillation limited to $2V_{CC}$. After simplifying terms in an exponential series the following can be derived:

$$-A\omega^2\cos(\omega t)$$

$$+\frac{I_s\exp\left(\frac{V_B}{V_T}\right)A\left(\frac{C_1}{V_T\left(C_1+C_2\right)}\right)\omega}{C_{tot}}\sin(\omega t)\times\left(\frac{-1}{I_s\exp\left(\frac{V_B}{V_T}\right)R_P} + \sum_{n=0}^{\infty}\left(\frac{C_1}{V_T\left(C_1+C_2\right)}\frac{-A\cos(\omega t)}{n!}\right)^n\right)$$

$$+A\cos(\omega t)\left(\frac{1}{C_{tot}L}\right) = 0$$

$$\tag{A2}$$

20

The first harmonic is then equated to zero. The terms $\sin(\omega t)$ and $\cos^{2n+1}(\omega t)$ are both odd terms, with $\cos^{2n}(\omega\tau)$ being an even term. The multiplication of two odd terms results in an even term, and odd terms multiplied by even terms are odd. The first harmonic is under consideration and therefore to simplify the equations, terms containing the multiplication of even and odd terms are considered. This approach leads to (A1) defining the oscillation frequency and amplitude for the oscillator. For the solution of (A3), only the first harmonic term is considered and the equation can be rewritten as in (B1). This yields a slight overestimate, assuming V_B is below the bandgap voltage of the process. For larger bias voltages the non-linearity becomes large and higher order harmonics are necessary to estimate the oscillator's FOM accurately. This is the bias voltage and sets the bias current of the active transistor. For V_B greater than the bandgap voltage plus $2V_T$ the oscillation frequency is predicted to be 1.8% more than the resonant frequency of the tank circuit, which is the oscillation frequency anticipated for an oscillator that is in the voltage-limited regime. This point has been demonstrated to yield optimal conditions for phase noise performance in an oscillator. The transistor model is simplified and the base-to-collector current is ignored. This is a valid assumption if the transistor is in the region of being current-limited or in the early voltage limited area.

$$-\omega^2 \cos(\omega t)$$
$$+\frac{I_s \exp\left(\frac{V_B}{V_T}\right)\omega}{C_{tot}} \times \left(\frac{-1}{I_s \exp\left(\frac{V_B}{V_T}\right)R_P}\sin(\omega t) + \sum_{n=0}^{\infty}\left(K_1\left(K_1\frac{A}{(2n)!}\right)^{2n} \times \left(\frac{1}{2^{2n}}\left(\binom{2n}{n}\sin(\omega t) + (K_3 + K_4 + ... K_5)\right)\right)\right)\right)$$
$$+\cos(\omega t)\left(\frac{1}{C_{tot}L}\right) = 0$$

$$(A3)$$

Where $K_3 = \binom{2n}{n-1}\left(\sin(\omega t - 2\omega t) + \sin(\omega t + 2\omega t)\right)$,

$$K_4 = \binom{2n}{n-3}\left(\sin(\omega t - 4\omega t) + \sin(\omega t + 4\omega t)\right),$$

$$K_5 = \binom{2n}{0}\left(\sin(\omega t - (2n)\omega t) + \sin(\omega t + (2n)\omega\tau)\right).$$

7   Appendix B

To solve for the new variables, (13) and (14) are solved. The solution to (13) is approached in a similar fashion as before. The solution of (14) is assumed to have the form:

$v_E = A_1 \cos(\omega t) + A_2 \cos(2\omega t)$ and $v_1 = A \cos(\omega t)$, and I_{CONST} is set by the bias conditions. Substituting these values into (15) and (16) and then solving simultaneously for the variables A_1, A_2, ω, and A lead to the following set of equations:

$$
\begin{aligned}
\left(-A_1 \omega \sin(\omega t) - A_2 2\omega \sin(2\omega t)\right)\left(C_1 + C_2\right) = \\
-C_1 A\omega \sin(\omega) - I_{CONST} + \\
I_s \exp\left(\frac{V_B}{V_T}\right)\left(1 + \frac{A_1^2}{4V_T^2} + \frac{A_2^2}{4V_T^2} - \frac{A_1^2 A_2}{8V_T^3}\right) + \\
I_s \exp\left(\frac{V_B}{V_T}\right)\left(\frac{A_1^2 A_2^2}{8V_T^4} + \frac{A_1 A_2}{2V_T^2} - \frac{A_1}{V_T} - \frac{A_1 A_2^2}{4V_T^3}\right)\cos(\omega t) + \\
I_s \exp\left(\frac{V_B}{V_T}\right)\left(\frac{A_1^2 A_2^2}{8V_T^4} + \frac{A_1^2}{4V_T^2} + - \frac{A_2}{V_T} - \frac{A_1^2 A_2}{4V_T^3}\right)\cos(2\omega t)
\end{aligned}
\tag{B1}
$$

which leads to three separate equations:

$$
I_s \exp\left(\frac{V_B}{V_T}\right)\left(1 + \frac{A_1^2}{4V_T} + \frac{A_2^2}{4V_T} - \frac{A_1^2 A_2}{8V_T^2}\right) - I_{CONST} = 0
\tag{B2}
$$

$$
\left(C_1 A\omega - \left(C_1 + C_2\right)A_1 \omega\right) = \left(I_s \exp\left(\frac{V_B}{V_T}\right)\left(\frac{A_1^2 A_2^2}{8V_T^4} + \frac{A_1 A_2}{2V_T^2} - \frac{A_1}{V_T} - \frac{A_1 A_2^2}{4V_T^3}\right)\right)
\tag{B3}
$$

$$
I_s \exp\left(\frac{V_B}{V_T}\right)\left(\frac{A_1^2 A_2^2}{8V_T^4} + \frac{A_1^2}{4V_T^2} + - \frac{A_2}{V_T} - \frac{A_1^2 A_2}{4V_T^3}\right)\cos(2\omega t) = -A_2 2\omega \sin(2\omega t)\left(C_1 + C_2\right)
\tag{B4}
$$

Equations (B1) to (B4) are only valid for small values of A_1 and A_2. The error in the truncated exponential function also results in large errors when using (B3) and (B4) to estimate the oscillation frequency. The equations do however provide a good basis for the estimation of the ratio of A_1/A_2. The result from (B5) shows that the average current into the emitter is a function of the emitter voltage, not just the bias current. Increasing the feedback voltage will increase the average current, and the associated shot noise of the bias current. The first harmonic of the collector current is not limited by the

bias current and will continue to increase as the emitter feedback voltage is increased. To investigate the oscillation frequency more accurately, equation (B4) is considered. The equation can be expanded using (B5). The exponential term is separated into even and odd components as before. The result is given by (24).

$$\left(\frac{A}{L \| R_P} + C_2 A_1 \omega^2\right) \cos(\omega t) =$$

$$P\omega\left(\left(A_1\left(T_1 T_2\right)\right) + \left(A_2 T_2 T_3\right) - A_2 T_4 T_1 - A_2 T_5 T_1 - \left(\frac{A_1}{4}\right) T_6 T_4 + \left(\frac{A_1}{4}\right) T_6 T_5\right) \sin(\omega t) +$$

$$P\omega\left(\frac{A_2}{2} T_6 T_4 + \frac{A_2}{2} T_6 T_5 - A_2 2 T_2^2 + \left(\frac{A_1}{2}\right) T_1 T_3 - \frac{A_1}{2} T_4 T_2 - \frac{A_1}{2} T_5 T_2\right) \sin(2\omega t)$$

(B5)

with the coefficients defined by:

$$T_1 = \sum \left(\frac{A_1^{2n}}{2^{2n}\left((2n)! V_T\right)^{2n}} \binom{2n}{n} \left(\frac{1}{n+1}\right)\right),$$

$$T_2 = \sum \frac{A_1^{2n}}{2^{2n}\left((2n)! V_T\right)^{2n}} \binom{2n}{n},$$

$$T_3 = \sum \frac{A_1^{2n}}{2^{2n}\left((2n)! V_T\right)^{2n}} \left(\binom{2n+1}{n}\right),$$

$$T_4 = \sum_{n=0}^{\infty} \left(\left(\frac{A_1}{(2n+1)! V_T}\right)^{2n+1} \frac{1}{2^{2n}} \left(\binom{2n+1}{n}\right)\right),$$

$$T_5 = \sum_{n=0}^{\infty} \left(\left(\frac{A_1}{(2n+1)! V_T}\right)^{2n+1} \frac{1}{2^{2n}} \binom{2n+1}{n-1}\right), \text{ and}$$

$$T_6 = \sum_{n=0}^{\infty} \left(\left(\frac{A_1}{(2n+1)! V_T}\right)^{2n+1} \frac{1}{2^{2n}} \left(\binom{2n}{n}\left(\frac{4n+2}{(n+1)(n+2)}\right)\right)\right).$$

The result of the analysis is that the amplitude of A_1 relative to A, the oscillation amplitude, is not equal to $A\left(\frac{C_2}{C_2 + C_1}\right)$.

23

References

[1] A. Demir, A. Mehrotra, J. Roychowdhury, "Phase noise in oscillators: A unifying theory and numerical methods for characterization", IEEE Transactions on Circuits and Systems I: Fundamental Theory and Applications, vol. 47, no. 5, pp. 655-674, May 2000.

[2] S. K. Reynolds, B. A. Floyd, U. R. Pfeiffer, T. Beukema, J. Grzyb, C. Haymes, B. Gaucher, M. Soyuer, "A silicon 60-GHz receiver and transmitter chipset for broadband communications", IEEE Journal of Solid-State Circuits, vol. 41, no. 12, pp. 2820-2830, December 2006.

[3] P. Andreani, A. Bonfanti, L. Romanò, C. Samori, "Analysis and design of a 1.8-GHz CMOS LC quadrature VCO," IEEE Journal of Solid-State Circuits, vol. 37, no. 12, pp. 1737–1747, December 2002.

[4] A. Buonomo, M. P. Kennedy, A. Lo Schiavo, "On the synchronization condition for superharmonic coupled QVCOs", IEEE Transactions on Circuits and Systems—1: Regular Papers, vol. 58, no. 7, pp. 1637-1646, July 2011.

[5] J. Liua, Ji. Jiangb, X. Zhoua, "A low phase noise and low spur PLL with auto frequency control circuit for L1-band GPS receiver", Microelectronics Journal, vol. 46, no. 7, pp. 617–625, July 2015.

[6] Y. Sun, F. Herzel, L. Wang, J. Borngraber, W. Winkler, R. Kraemer, "An integrated 60 GHz receiver front-end in SiGe:C BiCMOS," Proc. Silicon Monolithic Integr. Circuits RF Syst. Top. Meeting Dig., pp. 269–272, January 2006.

[7] R. Aparicio, A. Hajimiri, "A noise-shifting differential Colpitts VCO", IEEE Journal of Solid-State Circuits, vol. 37, no. 12, pp. 1728-1736, December 2002.

[8] M. Bagheria, A. Ghanaatiana, A. Abrishamifara, M. Kamarei, " A cross coupled low phase noise oscillator using an output swing enhancement technique", Microelectronics Journal, vol. 45, no. 8, pp. 1008-1013, August 2014.

[9] D. Li, Y.-T. Yang, Z.-M. Zhu, Z.-C. Shi, "A 5-GHz LC VCO with digital AAC and AFBS for 2.4 GHz ZigBee transceiver applications",

Microelectronics Journal, vol. 46, no. 6, pp. 415–421, June 2015.

[10] A. Demir, "Phase noise in oscillators: DAE's and colored noise sources," in Proc. IEEE/ACM Int. Conf. CAD, November 1998.

[11] P. Vanassche, G. Gielen, W. Sansen, "Efficient analysis of slow-varying oscillator dynamics", IEEE Transactions on Circuits Systems I, Regular Papers, vol. 51, no. 8, pp. 1457–1467, August 2004.

[12] A, Kourania, E. Hegazib, Y. Ismaila, "A 76.8 MHz temperature compensated MEMS reference oscillator for wireless handsets", vol. 46, no. 6, pp. 496–505, June 2015.

[13] A. Beléndez, E. Gimeno, M. L. Alvarez, D. I. Méndez, "Nonlinear oscillator with discontinuity by generalized harmonic balance method", Computers & Mathematics with Applications, vol. 58, no. 11–12, pp. 2117-2123, December 2009.

[14] A. Hajimiri, H. L. Thomas., "The Design of Low Noise Oscillators", Kluwer, 2000, ch. 3, pp. 17-31.

[15] A. Beléndez, A. Hernández, T. Beléndez, M.L. Álvarez, S. Gallego, M. Ortuño, C. Neipp, "Application of the harmonic balance method to a nonlinear oscillator typified by a mass attached to a stretched wire", Journal of Sound and Vibration, vol. 302, no. 5, pp. 1018-1029, November 2007.

[16] A. Demir, J. Roychowdhury, "A reliable and efficient procedure for oscillator PPV computation, with phase noise macromodeling applications", IEEE Transactions on Computer-Aided Design of Integrated Circuits and Systems, vol. 22, no. 2, pp. 188-197, February 2003.

[17] S. Perticaroli, F. Palma, "Design criteria based on Floquet eigenvectors for the class of LC-CMOS pulsed bias oscillators", Microelectronics Journal, vol. 44, no. 1, pp. 58-64, January 2013.

[18] A. Tasic, W. A. Serdijn, and J. R. Long, "Spectral analysis of phase noise in bipolar LC-oscillators: Theory, verification, and design," IEEE Transactions on Circuits Systems I: Regular Papers, vol. 57, no. 4, pp.

737–751, April 2010.

[19] B. van der Pol, "The nonlinear theory of electric oscillations", Proceedings of the Institute of Radio Engineers, vol. 22, no. 9, pp. 1051-1086, September 2006.

[20] S. Rong, H. C. Luong, "Analysis and design of transformer-based dual-band VCO for software-defined radios", IEEE Transactions on Circuits and Systems — 1: Regular Papers, vol. 59, no. 3, pp. 1-15, March 2012.

[21] S. I. J. Gierkink, S. Levantino, R. C. Frye, C. Samori, V. Boccuzzi, "A low-phase-noise 5-GHz CMOS quadrature VCO using superharmonic coupling", IEEE Journal of Solid-State Circuits, vol. 38, no. 7, pp 1148-1154, July 2003.

[22] F-R. Liao, S-S. Lu, "30 GHz transformer-coupled and reused injection-locked VCO/divider in 0.13 μm CMOS process", IET Electronics Letters, vol. 44, no. 10, pp. 625-626, January 2006.